Double system wave energy converter for the breaker zone

In this paper a particular type of wave energy converter, namely EDS (Energy Double System) is presented. It is a two-body point absorber composed by a heaving float and a surging paddle, mounted on the same structure and aligned along the wave propagation direction. The system is designed for working in the breaker zone, where waves close to breaking can generate a considerable surging force on the paddle.
A scale EDS model has been built and tested in the wave flume of the Hydraulics Laboratory of the Politecnico di Milano. The power absorbed by the system, varying its configuration, distance from the shoreline and wave, has been measured, and interesting efficiencies have been found.

■ *S. Malavasi, M. Negri*

Introduction

After more than forty years since its beginning, scientific research in wave energy harnessing still continues nowadays: the great availability of wave energy on the coasts of the world is continuously pushing scientists and the engineering community to study new methods and invent new machines for wave energy harvesting, with the hope to establish one or more technologies that are economically feasible. Unlike wind energy, where the technology of wind turbines is well established, for wave energy no system has reached the commercial state, despite the fact that several different prototypes have been placed in the sea: just to mention a few, Wavestar, Oyster, Pelamis, Limpet, AquaBuOY, Wave Dragon and many others. In the reference literature,

this great variety of technologies are classified according to the type of operation of the WECs (point absorber, attenuator, terminator, oscillating water columns, overtopping) and their positioning (offshore, nearshore, shoreline); reviews of wave energy technology can be found in the works of Falnes [1], Falcao [2], López *et al*. [3].

Research on wave energy has been developed mainly in northern Europe, also owing to the highly energetic seas that characterize this zone. Lately, also less energetic seas are being considered for wave energy harvesting, like the Italian coasts, which are characterized by power ranging from 2 to 10 kW m⁻¹ (Vicinanza *et al*. [4]); in Bozzi *et al*. [5] a simulation of wave energy production in various Italian sites is made, and it is shown that fairly good results are obtainable if ocean WEC are downscaled according to the wave climate.

Recently, researchers have paid some attention on the nearshore region, because it seems to be a good compromise between structure costs and energy availability, which can be a large part of the correspondent offshore one (Folley and Whittaker

■ **Contact: Marco Negri**
marco.negri@polimi.it

[6]); furthermore, the nearshore region has the advantage of natural concentration of wave direction and storm filtering.

In this work, we present the experimental analysis of the behavior of a particular wave energy converter designed for the breaker zone. The tests we present were performed in the wave flume of the Hydraulics Laboratory of Politecnico di Milano.

The peculiarity of this WEC, called EDS (Energy Double System), is to harness wave energy in the breaker zone, shortly before waves break. This position allows the energy harvesting before the dissipation due to the wave breaking, moreover it reduces the cost of installation and maintenance of the device. An optimal solution could be installing the EDS on existing structures like piers and breakwaters. The use of a nearshore WEC agrees with what discussed in [6], where it is shown how energy dissipation by bottom friction can be small if bottom slope is some high, and so a relevant part of offshore wave energy can reach shallow waters (5-10 m, depending on the wave dimension). Furthermore, in [7] it is shown that the surge force is considerably higher in the nearshore region than offshore.

The possibility of harnessing both the high surge wave force that characterizes the nearshore zone and the still present heave wave force led to the design of a wave energy converter with two different oscillating bodies, a surging paddle and a heaving float, held by the same arm, which is pivoted over the free surface (Fig. 1). The EDS system draws inspiration from the Wavestar machine (Hansen *et al.* [8], www.wavestarenergy.com), and it mainly differs
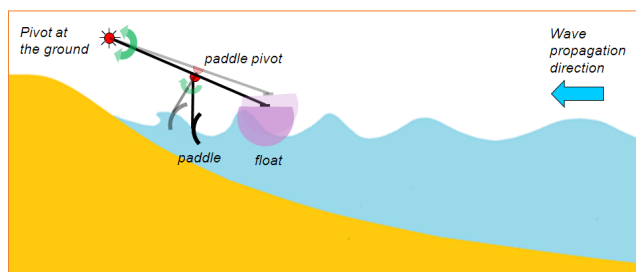
for the presence of the paddle, and in that the arm holding the float is aligned along the wave direction propagation, instead of perpendicular to it.

Experimental Setup

The EDS lab model was realized at 1:25 scale (see scheme in Fig. 2). The main arm $\overline{AB}$, pivoted over the free surface in point O, supports the float and the paddle on the right side. The A point of fastening between the float and the main arm is rigid. The float PTO, a heaving disc immersed in oil, is connected through a leverage in point B.

The arm $\overline{CE}$, pivoted on the main arm in point C, holds the paddle. The paddle PTO, again a heaving disc immersed in oil, reacts against the paddle arm in D and the main arm in F.

The system has two degrees of freedom, which we indicate as x_1 and x_2, position of heaving disc with respect to their position at rest.

The float is hemispherical at the bottom and cylindrical in its upper part. The radius of the float is 0.2 m, and total height is 0.140 m.

The paddle has cylindrical shape, a chord of 0.12 m and a width of 0.2 m. The principal characteristics of the model are reported in Table 1. The moment of inertia of EDS was calculated considering the second degree of freedom x_2 as blocked.
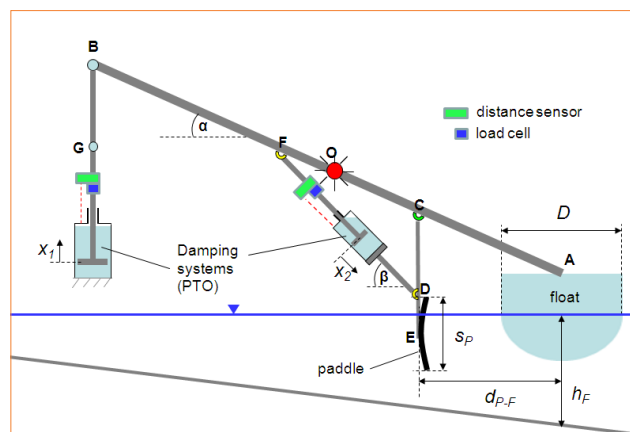

FIGURE 1 Scheme of the EDS wave energy converter

FIGURE 2 Scheme of the EDS lab model

Float arm length	OA [m]	0.4
Damper arm length	OB [m]	0.45
Diameter of the float	D [m]	0.2
Float static draft	d_F [m]	0.055-0.060
Moment of inertia	I [kg·m²]	0.30
Main arm inclination	α [°]	24°-26°
Paddle chord	s_p [m]	0.12
Paddle draft	d_p [m]	0.09
Inclination of paddle PTO	β [°]	35-45°

TABLE 1 Some characteristics of the EDS scale model

In Figure 3 the front part of the EDS is reported. The paddle PTO is visible. As mentioned before, the PTOs of paddle and float are heaving discs immersed in oil. In Figure 4 the scheme of the PTO systems of float and paddle are reported. Each PTO was equipped with a load cell and a sensor distance, in order to measure the position of the disc and the force exerted on it. The float damper (Fig. 4a) is a single disc, held by a stem that can slide through bearings fixed to the cylinder top, the cylinder being in turn fixed to the ground. To obtain a different amount of damping, different sizes of the disc have been used. The paddle damper is similar, except for two characteristics. Firstly, the stem supports two discs, a porous one which is fixed on the stem, and one that can slide along the stem for a short dis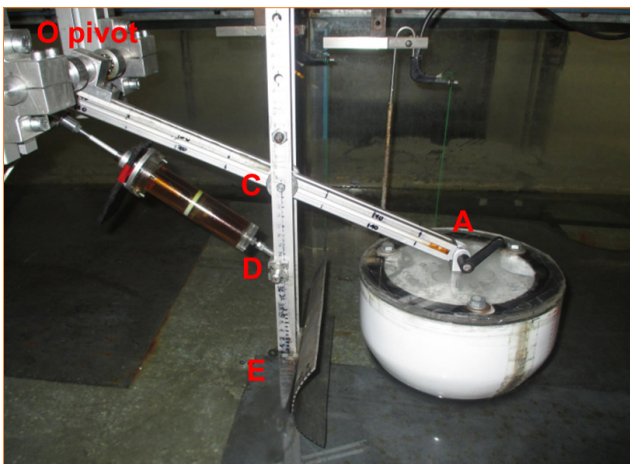tance (Fig. 4b). This solution allows to have different damping levels along the two directions of the stem movement: as the paddle receives the positive force from the wave, the stem is pushed into the cylinder and the two discs quickly approach, closing the holes of the fixed porous disc. The two discs remain attached until the motion is reversed, that is when the paddle gets back to its position. In that phase, the discs are detached, so the holes of the fixed disc are freed. In this way, during the wave push a major damping is generated on the paddle with respect to the return phase. However, it was also possible to generate a similar damping in the two directions of movement by tightening the two discs together. The other difference between float and paddle PTOs is that the latter reacts against the main arm in point F and not against the ground.

The amount of energy dissipated by the disc during an oscillation period T was calculated as:
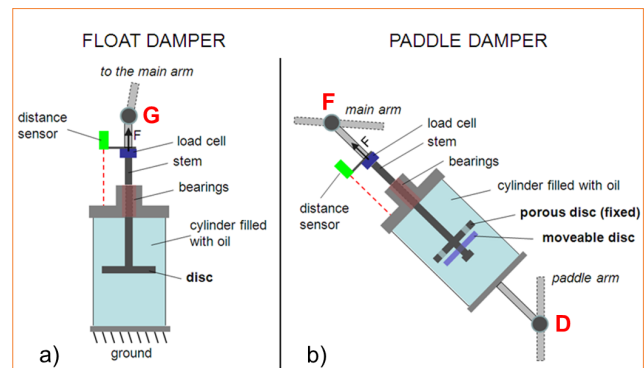
$$E = \int_T F_D \dot{x}\, dt$$

FIGURE 3 Front part of EDS lab model

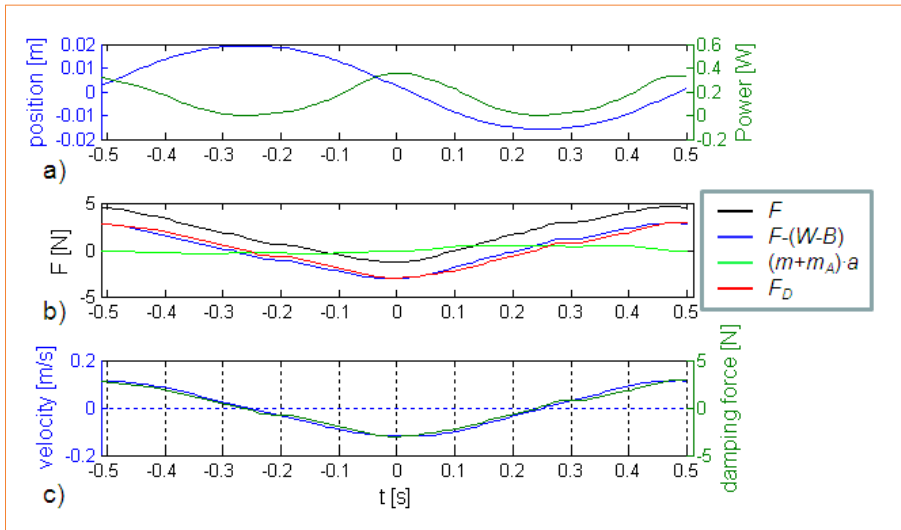**FIGURE 4** PTOs of float (a) and paddle (b)

FIGURE 5 Float PTO dynamics during a cycle of oscillation: a) disc position and dissipated power; b) forces on the disc; c) disc velocity and damping force

The average power absorbed by the EDS was calculated as the ratio between the total energy absorbed by the system in one period and the period duration.

$$P_{out} = \frac{E_1 + E_2}{T}$$

Where E_1 is the energy absorbed by the float and E_2 is the energy absorbed by the paddle. In Figure 6 an example of the instantaneous power absorbed in an oscillation cycle of the EDS is reported. The colors represent the different motion phases of float and paddle. The absorbed energy is also reported.

Where F_D is the damping force of the disc and v is the relative velocity between the disc and the cylinder that contains the oil. The damping force F_D was calculated from the total force F recorded by each load cell, by subtracting the inertial and gravitational contributions:

$$F_D(t) = F(t) - (m + m_A)\ddot{x}(t) - \left[W - B(x(t))\right]$$

Where m is the mass of the objects attached below the load cell, m_A is the disc added mass, W is the weight of the objects attached below the load cell, B is the buoyancy of the immersed objects in oil. As an example, in Figure 5 the dynamic parameters of the float PTO during an oscillation cycle is reported. Fig. 5a reports the relative disc position x and the power dissipated by the disc, Figure 5b reports the total force F measured by the load cell and its contributions, Figure 5c reports disc velocity and damping force F_D.
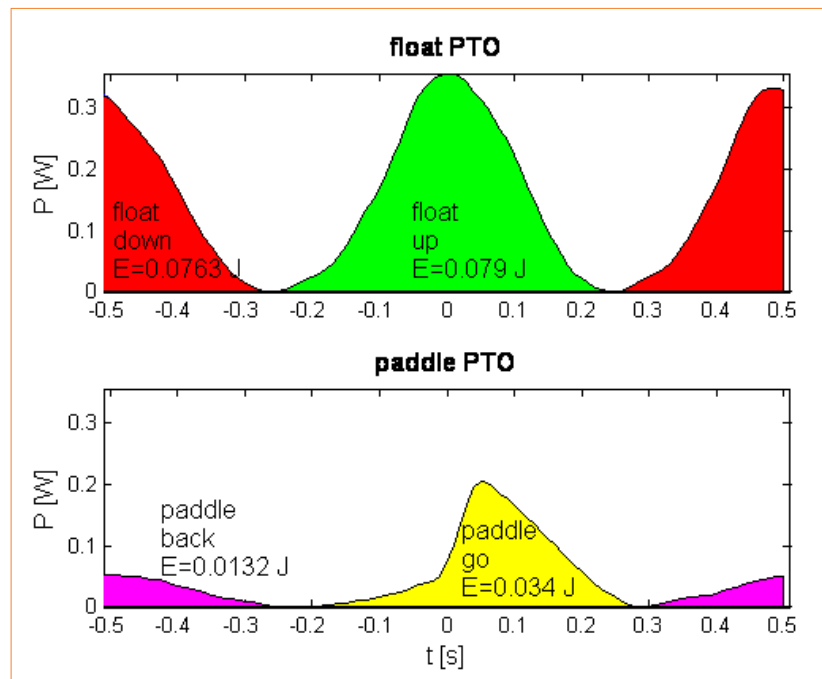

FIGURE 6 Instantaneous power dissipated by float and paddle PTOs

The damping generated by the PTO systems was not linear, and equivalent linear damping was calculated. With the approximation of considering the float motion vertical and the paddle motion horizontal, we calculated an equivalent vertical linear damping in point A for the float, and an equivalent horizontal linear damping in point E for the paddle. Furthermore, two values of equivalent linear damping were calculated for the paddle, one for the go-motion and the other for the back-motion. Expressions are reported below.

$$b_{1eq} = \frac{E_1}{\frac{T}{2}\omega^2 A_{x1}^2} \frac{\overline{OB}}{\overline{OA}}$$

$$b_{2eq-go} = \frac{E_{2-go}}{\frac{T}{4}\omega^2 A_{x2}^2} \frac{\overline{CD}}{\overline{CE}} \cos\beta$$

$$b_{2eq-back} = \frac{E_{2-back}}{\frac{T}{4}\omega^2 A_{x2}^2} \frac{\overline{CD}}{\overline{CE}} \cos\beta$$

Where A_{x1} and A_{x2} are the oscillation amplitudes of the heaving discs and

$$\omega = \frac{2\pi}{T}$$

The EDS was tested in a 30 m long and 1 m wide wave flume, equipped with a piston wave maker. The water depth inside the flume was 0.4 m. At the end of the flume a constant slope beach was installed. The slope of the beach was 1:8.25.

Three monochromatic waves were used to test the model; their properties were measured by two capacitive wave gauges, without the EDS model in the channel. Waves were measured on the beach and in the middle part of the channel with water depth h=0.4 m. Wave measurements in the middle part of the channel were analyzed by separating the incident and reflected waves according to the method of Goda and Suzuki [9]. We found a nearly constant reflection coefficient for the three waves considered. In Table 2 wave properties in water height h = 0.4 m are reported.

Wave power per unit width crest was calculated from linear theory, considering $H = 2a_I$ the reference wave height:

$$P_I = \frac{1}{8}\rho g H^2 c_g$$

Group celerity c_g was calculated as:

$$c_g = \frac{c}{2}\left(1 + \frac{2kh}{\sinh(2kh)}\right)$$

With $c = L/T$ being wave celerity, k the wave number and h the water depth.

The efficiency of the system CWR (capture width ratio) was calculated as:

$$CWR = \frac{P_{out}}{P_I D}$$

The efficiency is referred to the incident wave power P_I and not to the actual wave power, which may be minor and change along the beach. It follows that the EDS efficiency is calculated on the basis of a somehow "offshore wave energy" (more correctly, wave energy in a non-dissipative zone, since water depth in the channel is not deeper).

The wave height measured on the beach is reported in Figure 7 for the three waves. For wave B and wave C, a steep rise of height can be seen for $h/D = 0.4$, that is a sign of incipient breaking. Wave height relative maxima can be seen at $h/D = 0.8$, 1.3, 1.8 for wave A, $h/D = 1.5$ for wave B, at $h/D = 1.5$ and 1.9 for wave C.

The experiments were conducted in stationary condition, that means that only the part of the signals where waves and oscillations of the EDS were stabilized were considered for the subsequent analysis. All the acquired signals, *i.e.* positions of the

Wave id	a_I [mm]	a_R [mm]	T [s]	L [m]	P_I [W/m]	r [%]
Wave A	24.4	1.6	1.02	1.52	2.70	6.4
Wave B	25.4	1.6	1.36	2.29	3.97	6.2
Wave C	31.7	2.1	1.20	1.92	5.45	6.8

TABLE 2 Wave properties in water height h=0.4 m
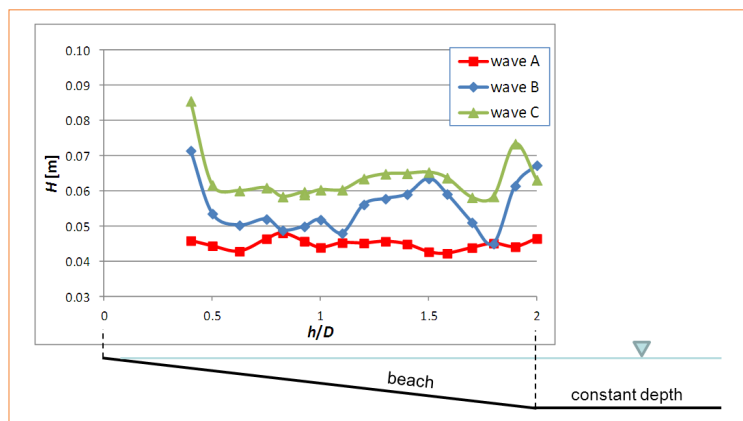
FIGURE 7 Wave height along the beach

of the EDS for wave A is quite influenced by the parameters that characterize the EDS, whereas for wave B and wave C the efficiency is less sensitive to these changes. This is due to the fact that wave A has the shortest period, and it should be the closest to natural periods of the EDS.

For all the three waves, it can be seen that CWR fairly follows the trend of H.

The best value of float-paddle distance was the smallest tested, that is $d_{P-F}/D = 0.8$, for all the three waves. The

heaving discs, force exerted on heaving discs, and water elevation were phase averaged on the basis of the wave period.

Results

Many geometrical and mechanical parameters characterize the EDS. In this work, we considered the influence of some of them, keeping the others constant. The parameters that varied through the tests were: distance between paddle and float, float external damping and water depth at the float. The fixed parameters were the moment of inertia of the structure, paddle damping in the two directions, paddle immersion at rest. The moment of inertia of the EDS was set as small as possible, given the physical limitation of the model scale. Paddle damping was set to a reasonable value. The paddle immersion at rest d_P was 0.09 m. This value was found to be the optimal one in the previous work of Negri *et al.* [10]. Paddle damping was set to about 15 Nsm^{-1} in the shoreward motion and about 5 Nsm^{-1} in the seaward motion.

In Figure 8 efficiency of the EDS system is reported as a function of water depth at the float, float external damping (circle dimension), distance between paddle and float (line color). Wave height is also reported as a function of water depth. The efficiency
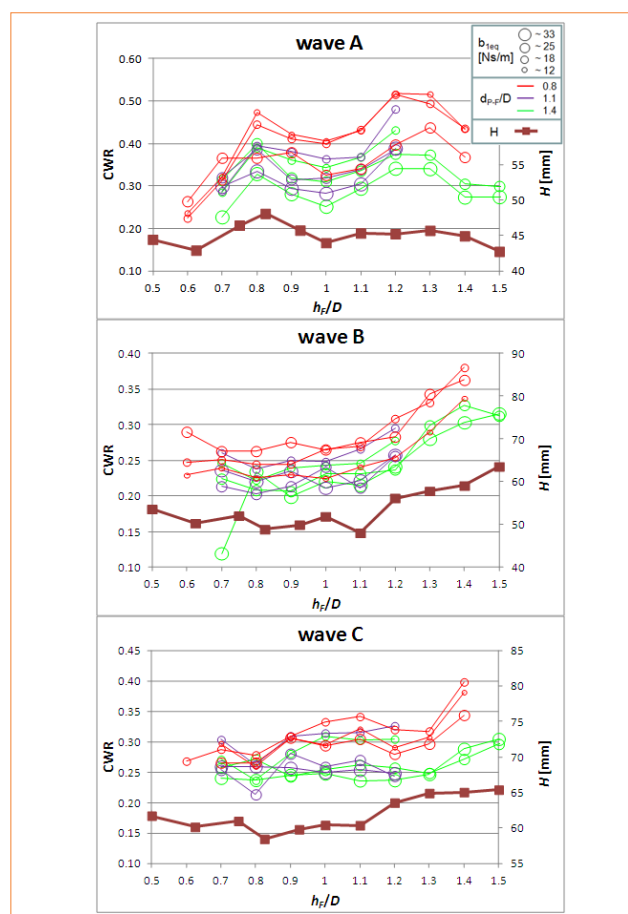

FIGURE 8 Efficiency of the EDS depending on float external damping, distance between paddle and float, and water depth at the float

worst configuration was $d_{P-F}/D = 1.1$, even if there was not much difference with $d_{P-F}/D = 1.4$.

For wave A, it can be seen that the effect of float damping on the efficiency is almost independent from the other two parameters: indeed, best damping is almost always the small value tested, regardless of paddle-float distance and water depth; only for $h_F/D < 0.8$, higher efficiency is obtained with a higher float external damping. For wave A, the highest efficiencies were obtained with the smallest float damping we tested $b_{1,eq} = 12$ Nsm^{-1}; it was not possible to reach the optimal float damping, due to the physical limitation on the amplitude of motion of the heaving disc.

For wave B, optimal float damping changes with paddle-float distance: for $d_{P-F}/D = 0.8$, optimal damping is 25 Nsm^{-1}, whereas for the other two distances the optimal damping is less, $b_{1,eq} = 18$ Nsm^{-1}.

For wave C the optimal damping is almost always 18 Nsm^{-1}, regardless of the paddle-float distance.

It is interesting to see how the absorbed EDS power is subdivided between the float and the paddle. In Figure 9 the partial efficiency of the float, further divided into upward and downward motion, and the paddle, further divided into shoreward and seaward motion (go- and back-motion), are reported. For the three waves, configuration with $d_{P-F}/D=0.8$ and float external damping $b_{1eq} = 12, 25, 18$ Nsm^{-1}, respectively, are reported. They are the best configurations found for each wave, except from some isolated points discussed before.

Fig. 9 shows how float efficiency increases and paddle efficiency decreases as water depth increases.

For low depth ($h_F/D = 0.6$-0.7), paddle efficiency is about half the total efficiency, while it becomes a third or minus as depth increases. The reduction of paddle efficiency in deep water is due to the reduction of surge force and to the greater linearity of the waves: a light paddle, which is not resonant with the waves, works better with shallow-water waves, because they have shoreward transport mass. Float efficiency individually taken follows the trend of total efficiency. Float efficiency is quite evenly distributed between the upward and downward motion, however some differences can be noted;
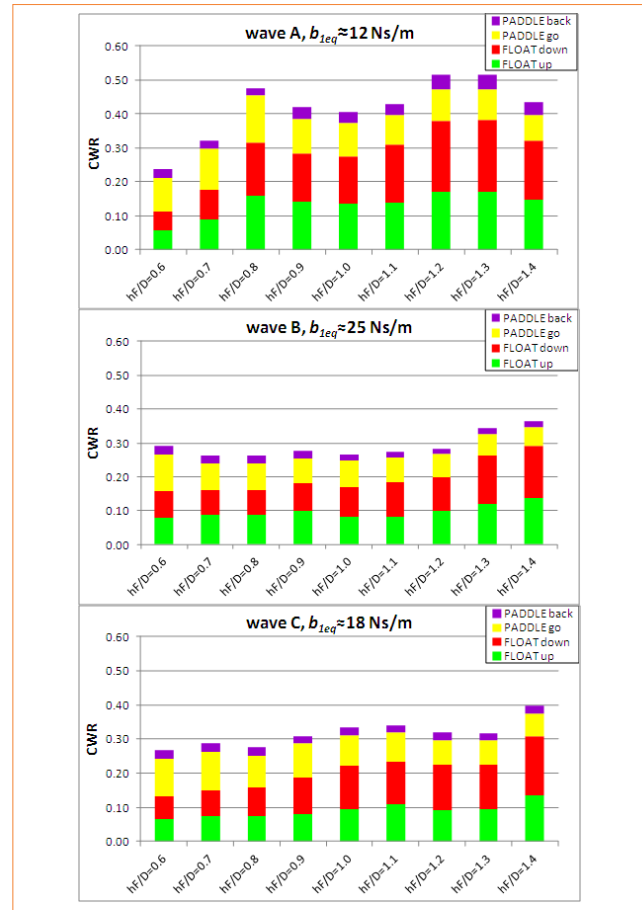
they are generated by the non-linearity of both the external damping and the shallow water waves. The energy absorbed by the paddle in the go-phase is much higher than in the back-phase, because of the aforementioned mass transport of the waves.

Conclusions

The potential of the EDS, a multi-body WEC composed by a heaving float and a surging paddle, has been analyzed in this work. The EDS scale model has been tested in a wave flume, at

various depths along a constant slope beach and in various configurations, varying some of the main parameters that characterize the system. The system has been tested with three monochromatic waves. The efficiency of the system was calculated on the basis of the wave power off the beach, making the results comparable with the ones about exploiting offshore wave energy. We found that the system efficiency is dependent on the distance from the shoreline. This is due to two reasons, which are linked to one another: water depth and wave height, that punctually is established along the beach. Wave height variation is due to the wave reflection over the beach. Efficiency peaks of the EDS occur where wave height peaks occur, more markedly for the smallest wave tested.

Generally, the efficiency of the float increases as water depth increases, while paddle efficiency decreases. The highest EDS efficiencies were found with the paddle close to the float, $d_{P\text{-}F}/D = 0.8$.

We found that optimal external damping of the float is generally independent from water depth and float-paddle distance.

The optimal damping of the float is almost independent from the paddle-float distance and the water depth.

The experimental efficiency measured is about 30%, increasing on average from shallow to deep waters. For the smallest wave the efficiency reached values up to 50% in a water depth $h_F/D = 1.1$.

Although the main EDS parameters were analyzed in this work, the characteristics of the paddle have yet to be optimized, especially as regards damping and shape. We are therefore confident that EDS efficiency will further increase.

Stefano Malavasi, Marco Negri
Politecnico di Milano, Department of Civil and Environmental Engineering (DICA), Italy

references

[1]   J. Falnes, A review of wave-energy extraction, in *Marine Structures*, 20, pp. 185-201, 2007.

[2]   A.F. de O. Falcao, Wave energy utilization: A review of the technologies, in *Renewable and Sustainable Energy Reviews*, 14, pp. 899-918, 2010.

[3]   I. López, J. Andreua, S. Ceballos, I. Martínez de Alegría, I. Kortabarria, A review of wave energy technologies and the necessary power-equipment, in *Renewable and Sustainable Energy Reviews*, 27, pp. 413-434, 2013.

[4]   D. Vicinanza, P. Contestabile, V. Ferrante, Wave energy potential in the north-west of Sardinia (Italy), in *Renewable Energy*, 50, pp. 506-521, 2013.

[5]   S. Bozzi, R. Archetti, G. Passoni, Wave electricity production in Italian offshore: A preliminary investigation, in *Renewable Energy*, 62, pp. 401-416, 2014.

[6]   M. Folley, T.J.T. Whittaker, Analysis of the nearshore wave energy resource, in *Renewable Energy*, 34, pp. 1709-1715, 2009.

[7]   M. Folley, T.J.T Whittaker, A. Henry, The effect of water depth on the performance of a small surging wave energy converter, in *Ocean Engineering*, 34, pp. 1265-1274, 2007.

[8]   R. H. Hansen, M.M. Kramer, E. Vidal, Discrete displacement hydraulic power take-off system for the Wavestar Wave Energy Converter, in *Energies*, 6, pp. 4001-4044, 2013.

[9]   Y. Goda, Y. Suzuki, Estimation of incident and reflected waves in random wave experiments, in *Marine Hydrodynamics Division Port and Harbour Research Institute*, Ministry of Transport Nagase, Yokosuka, Japan, 1976.

[10] M. Negri, F. Clerici, S. Malavasi, A breaker-zone wave energy converter, International Conference on Renewable Energies and Power Quality, ICREPQ'13, Bilbao, Spain, 2013.